RSC Advances




ROYAL SOCIETY OF CHEMISTRY

www.rsc.org/advances

RSC Advances

Cite this: DOI: 10.1039/c0xx00000x

www.rsc.org/xxxxxx



Full Paper

# Fabrication of Silica Nanoparticles based Polymer Nanocomposites via Combination of Mussel Inspired Chemistry and SET-LRP

**Chunning Heng[a,b], Meiying Liu[a], Ke Wang[c], Xiaoyan Zheng[b], Hongye Huang[a], Fengjie Deng[a], Junfeng Hui[b,*], Xiaoyong Zhang[a,*], Yen Wei[c,*]**

***Received (in XXX, XXX) Xth XXXXXXXXX 200X, Accepted Xth XXXXXXXXX 200X***
**DOI: 10.1039/b000000x**

A highly benign, simple and effective strategy was successfully developed for the first time for fabrication of hydrophilic thermo-responsive polymer modified silica nanoparticles ($SiO_2$-PDA-poly(NIPAM)) at low temperature and mild reaction conditions via combination of mussel inspired chemistry and SET-LRP. $SiO_2$ NPs were first modified with polydopamine (PDA), which was formed by self-polymerization of dopamine in rather mild conditions. The 2-bromo-2-methylpropionyl bromide was further covalently attached on the surface of PDA modified $SiO_2$ NPs. Afterward, the poly(NIPAM) was in situ grown on the surface of Br-containing $SiO_2$ NPs by SET-LRP method. Consequently, the surface of $SiO_2$-PDA nanoparticles is intrinsically covered by a layer of free poly(NIPAM) chains, which enable the poly(NIPAM) to be colloidally stable not only at room temperature, but also upon incubation in the presence of proteins under physiological conditions. After modifying with PNIPAM, the functional $SiO_2$ NPs remain the pristine structure, however their dispersibility was significantly improved in polar and nonpolar solution. As compared with previous methods, this strategy developed in this work is rather simple and effective. More importantly, due to the universality of mussel inspired chemistry, the novel strategy could also be used for surface modification of many other materials.

## 1. Introduction

In recent year, designed nanoparticles have been widely used in various fields and are also extensive foreground for pharmaceutical applications such as cell imaging, diagnosis and drug or gene delivery.[1-7] Nanoparticle-based techniques have shown great interest in biotechnology and biomedical applications, especially in ultrahigh throughput screening, electronic chip technology, multiple targets detection system, genetic diagnosis screening, and *in vitro* and *in vivo* diagnosis inside intact biologic systems.[8-15] Silica nanoparticles ($SiO_2$ NPs) are an important part of the nanomaterials, which are a kind of non-toxic, tasteless, no pollution of non-metallic materials.[12, 16-19] Owing to its optical transparency, chemical inertness, biological compatibility, $SiO_2$ NPs have shown a broad application prospect in cell markers, drug delivery, DNA transfection and selective separation.[20-22]

However, owing to the aggregation of $SiO_2$ NPs and poor dispersibility, the applications of $SiO_2$ NPs would be significantly restricted.[23, 24] So it is necessary to first modify the surface of $SiO_2$ NPs.[25, 26] It is well known that the Single-electron transfer living radical polymerization (SET-LRP) is an effective and simple way for surface modification.[27-36] As compared with classic ATRP, SET-LRP should be an alternative controlled living free radical polymerization, which can be occured at room temperature, air atmosphere and aqueous solution with rapid polymerization rate.[37-40] Given these advantages, SET-LRP has rapidly attracted great research attention and explored for various applications including the surface modification of carbon nanomaterials.[41-43] However, the bare $SiO_2$ NPs is lack of functional groups on their surface, the surface coating of $SiO_2$ NPs with silane derivatives and surface activation is required. These experimental procedure is relative complex, time consuming and high cost. It is therefore, development of novel surface modification of strategy is highly desirable for the development of $SiO_2$ NPs.

Mussel can hold fast to various substrates like rocks, metal, wood structure and marine organisms in tidal waves by secreting mussel foot proteins that form mussel byssus.[44, 45] When a suitable surface was found, mussel feet stretched out of the shell to secrete foot proteins, which after a curing process would form byssus consisting of proteinaceous thread and adhesive plaque.[46] Previous studies have shown that a catecholic amino acid called 3,4-dihydroxyphenyl-alanine (DOPA), which is formed by post-translational modification of tyrosine, makes up a major component of the mussel foot proteins and is crucial to achieving the remakable underwater adhesion, through various types of interactions including hydrogen bonding, metal-catechol coordination, electrostatic interaction, cation-π interaction and π-π aromatic interactions.[47-49] Inspired by this, a novel surface modification strategy has been developed by Lee *et al* in 2007.[50] They demonstrated that dopamine could mimic the function of mussel adhesion proteins (MAPs), which could self-polymerize under alkaline solution and form a polydopamine (PDA) coating.

The PDA coating could further reacted with amino and thiol functional groups through Michael addition reaction.[51-56] Because of its simplicity, universality and effectiveness, mussel inspired chemistry has emerged as a very useful surface functionalization strategy, which has been extensively explored for different applications recently.[57-61]

In this contribution, a novel method was developed for surface modification of $SiO_2$ NPs via combination of mussel inspired chemistry and SET-LRP. As shown in **Scheme 1**, the $SiO_2$ NPs were first coated with PDA via self-polymerization of dopamine under alkaline solution to obtain $SiO_2$-PDA. Then the Br-containing initiator (2-bromo-2 methylpropionyl bromide) was immobilized on $SiO_2$-PDA via reaction with the amino and hydroxyl groups on $SiO_2$-PDA. Finally, $SiO_2$-PDA-Br was utilized for surface polymerization of $SiO_2$-PDA-poly(NIPAM) via SET-LRP using NIPAM as the monomer. As compared with previous methods, this strategy could not only provide a universal and effective method for surface modification of $SiO_2$ NPs, but also offer the novel photothermal conversion capability of the final polymer nanocomposites.[62]

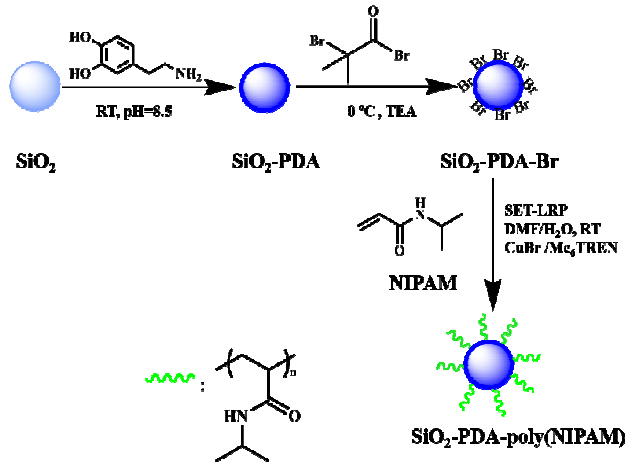


**Scheme 1.** Schematic representation for the synthesis of $SiO_2$-PDA-poly(NIPAM) via combination of mussel inspired chemistry and SET-LRP strategy. PDA films were first coated on the surface of pristine $SiO_2$ NPs via mussel inspired chemistry to obtain $SiO_2$-PDA. After that the initiator (2-bromo-2-methylpropionyl bromide) was further conjugated on $SiO_2$-PDA to obtain $SiO_2$-PDA-Br. Finally, the monomer (NIPAM) was further introduced on the surface of $SiO_2$-PDA-Br via SET-LRP.

## 2. Experiment

### 2.1 Materials and characterization

Tetraethyl orthosilicate (TEOS) was purchased from Sino Nanotech Ltd. (Beijing, China). Triethylamine (TEA, Aldrich, 99%), N, N-dimethylformamide (DMF, Aldrich, 99.8%), NIPAM ($M_W$: 113.16, 98%), CuBr, 2-bromo-2-methylpropionyl bromide (Aldrich, 98%), Tris(2-(dimethylamino)ethyl)amine ($Me_6TREN$) were purchased from Aladdin (Shanghai, China). tris (hydroxymethyl) aminomethane (Tris) is obtained from Sinopharm Chemical Reagent Co., Ltd. Dopamine hydrochloride was purched from Sangon Biotech. Co. (Shanghai, China). Transmission electron microscopy (TEM) images were recorded on a Hitachi 7650B microscope operated at 80 kV; the TEM specimens were made by placing a drop of the nanoparticle ethanol suspension on a carbon-coated copper grid. The Fourier transform infrared (FT-IR) spectra were obtained by using a Nicolet 380 Fourier transform spectrometer with a resolution of 2 $cm^{-1}$. The samples were pressed with KBr into a pellet before measuring the infrared absorption spectra. Thermal gravimetric analysis (TGA) was conducted on a TA instrument Q50 with a heating rate of 20 °C $min^{-1}$. Samples weight between 10 mg were heated from 25 to 600 °C in air flow (60 mL $min^{-1}$), $N_2$ as the balance gas (40 mL $min^{-1}$). Each sample was ultrasonicated for 30 min prior to analysis. The reported values are the mean values of three measurements. The X-ray photoelectron spectra (XPS) were performed on a VGESCALAB 220-IXL spectrometer using an Al Kα X-ray source (1486.6 eV). The energy scale was internally calibrated by referencing to the binding energy (*E*b) of the C1s peak of a carbon contaminant at 284.6 eV.

### 2.2 Preparation of $SiO_2$-PDA-Br

The steps to prepare uniform-size $SiO_2$ NPs as follows: First, 2.5 mL of TEOS and 27.5 mL of ethanol were added into a 250 mL conical flask, and mixture uniform. Then, 7.5 mL of ammonium and 22.5 mL of deionized water was rapidly poured out into above solution with stirring 24 h at room temperature. Later, the reaction mixture solution was separated by centrifugation at 7000 rpm for 20 min and washed with deionized water until removing unreacted raw materials. The obtained white solid was dried 12 h at 60 °C to acquired monodisperse $SiO_2$ NPs. The 100 mg ungroomed $SiO_2$ NPs and 100 mg of dopamine were put into 500 mL beaker. And then, 100 mL of Tris buffer solution (pH = 8.5) was poured into above beaker with ultrasonic vibrating for 10 min. The mixed solution was stirred at room temperature for 2 h and was separated from unreacted dopamine and Tris buffer solution by centrifugation at 7000 rpm for 10 min. The obtain brown solid was washed with distilled water for three times and dried at 50 °C for 10 h. Nextly, 100 mg of $SiO_2$ NPs, 10 mL of toluene and 10 mg of TEA were added to a 100 mL Schlenk flask and ice-water bath treatment for 10 min. 10 mg of 2-bromo-2-methylpropionyl bromide was mixed with 20 mL of toluene and was added dropwise into above reaction system under $N_2$ circumstance. The reaction was stirred at 0 °C for 4 h and the mixed solution was separated by centrifugation at 7000 rpm for 10 min. The obtained pruducts was washed with toluene for three times and dried 24 h at 40 °C in vacuum to give $SiO_2$-PDA-Br.

### 2.3 Preparation of $SiO_2$-PDA-poly(NIPAM)

The $SiO_2$-PDA-poly(NIPAM) was prepared using SET-LRP homopolymerization. 100 mg of $SiO_2$-PDA-Br, 1.58 g of NIPAM and 100 mg of CuBr were added to 50 mL Schlenk flask and purging with $N_2$. 15 mL dried DMF and 15 mL redistilled $H_2O$ were added into reaction system by a gastight syringe. 1 mL of $Me_6TREN$ was introduced by a gastight syringe followed by the reaction system set at 40 °C. And the polymerization reaction lasted for 24 h. The reaction mixture was separated by centrifugation at 7000 rpm for 10 min and washed with DMF and deionized water repeat three times. The obtained sample was dried 12 h at 40 °C in vacuum to obtain $SiO_2$-PDA-poly(NIPAM).

## 3. Results and discussion

**Fig. 1** shows the TEM images of the as-synthesized pristine $SiO_2$ NPs, modified $SiO_2$-PDA and $SiO_2$-PDA-poly(NIPAM). The as-

synthesized $SiO_2$ NPs are relatively uniform with an average particle size of 100 nm (**Fig. 1A** and **Fig. 1B**). Meanwhile, the $SiO_2$ NPs exhibit a near spherical morphology with a typical regular structure. As shown in **Fig. 1C** and **Fig. 1D**, similar to the results obtained from TEM studies, the diameter of $SiO_2$-PDA and $SiO_2$-PDA-poly(NIPAM) was increased as compared with nonmodified $SiO_2$ NPs. The particles are very clear because the surface of modified nanoparticles was wrapped with polymer coatings, which linked neighboring nanoparticles together. Furthermore, we can see that $SiO_2$-PDA exhibits superior dispersed ability and large-sized than pristine $SiO_2$ NPs. In general, the method described in this article is rather convenient and effective. More importantly, this surface functionalization method will not destroy the structure of $SiO_2$ NPs. Therefore, the physicochemical properties of $SiO_2$ NPs related to their structure can be well maintained after surface modification of $SiO_2$ NPs with polymers through the biomimic strategy.

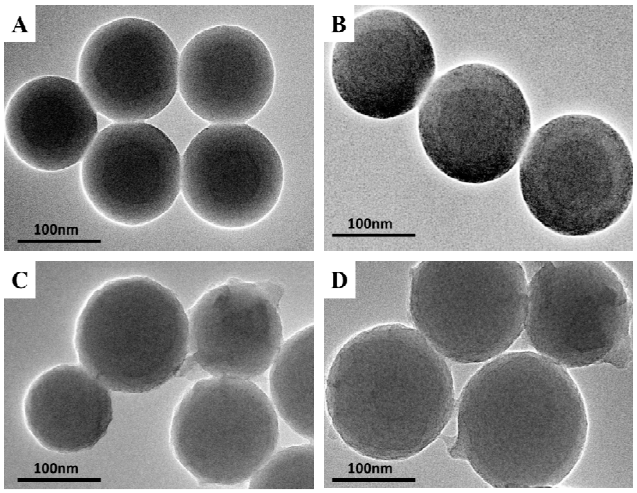


**Fig. 1** TEM images of original $SiO_2$ (A, B), $SiO_2$-PDA (C) and $SiO_2$-PDA-poly(NIPAM) (D), Thin polymer films coated on $SiO_2$ NPs were clearly viewed by TEM observation after they were functionalized with PDA and polymers. The TEM images confirmed the successful modification of NIPAM through mussel inspired chemistry and SET-LRP.

**Fig. 2** displays the FTIR spectra for the pristine $SiO_2$ NPs, $SiO_2$-PDA and $SiO_2$-PDA-poly(NIPAM). In pristine $SiO_2$ NPs, the stretching vibration of Si-O-Si at 1078.2 and 952.1 $cm^{-1}$ in the FT-IR spectrum of $SiO_2$ NPs. Moreover, after surface coated with PDA and NIPAM, the spectra of $SiO_2$-PDA and $SiO_2$-PDA-poly(NIPAM) exhibit some new absorption peaks which are not found in the spectrum of unmodified $SiO_2$ NPs. For example, the broad stretching bond of hydroxyl groups and amino group was closed to 3483.3 $cm^{-1}$, indicating that the successful coated $SiO_2$ NPs with dopamine. As compared with the $SiO_2$ NPs and $SiO_2$-PDA, a range of new absorption peaks were emerged in the sample of $SiO_2$-PDA-poly(NIPAM) due to the C-H stretching vibration of $CH_3$ (2964.5 $cm^{-1}$) and $CH_2$ (2860.2 $cm^{-1}$). In addition, the absorption peaks at around 1670.3 $cm^{-1}$ are assigned to the C=O and C-N bonds in poly(NIPAM) fixed on the surface of $SiO_2$ NPs.

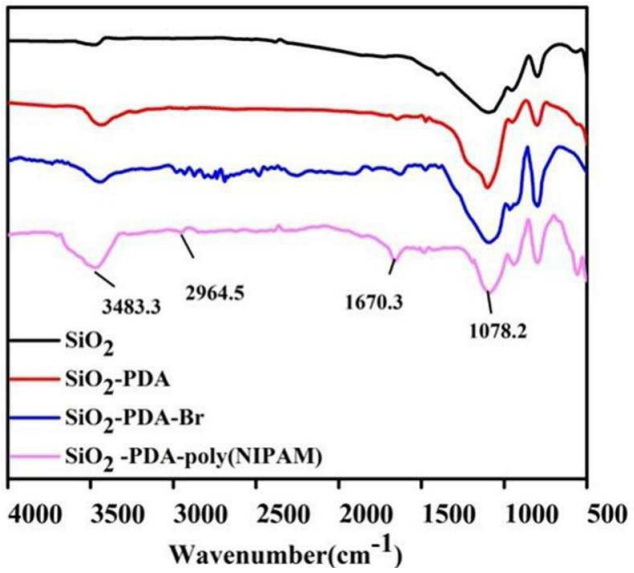


**Fig. 2** FT-IR spectra of $SiO_2$ NPs with NIPAM functionalized $SiO_2$ NPs. Characteristic IR peaks located at 1670.3, 2964.5 and 3483.3 $cm^{-1}$ were observed in $SiO_2$-PDA-poly(NIPAM), suggesting that the functional groups such as C=O, C-H and C-O were existed in $SiO_2$-PDA-poly(NIPAM).

A comparison of grafting amount for NIPAM grafted $SiO_2$ NPs was evaluated based on TGA results. The increment of mass loss could be considered as a reliable indicator of increasing grafting amount. **Fig. 3** shows the TGA curves of pristine $SiO_2$ NPs and all modified $SiO_2$ NPs. The mass loss of pristine $SiO_2$ NPs was primarily caused by the removal of residual water. An additional weight loss seen in modified silica nanoparticles can possibly be attributed to the thermal degradation of organic groups on the surface of $SiO_2$-PDA-poly(NIPAM). The thermal stability of ungroomed and modified $SiO_2$ NPs were evaluated by TGA (**Fig. 3A**). The differential thermal analysis (DTA) curves of $SiO_2$ NPs, $SiO_2$-PDA, $SiO_2$-PDA-Br and $SiO_2$-PDA-poly(NIPAM) are shown in **Fig. 3B-E**. As shown in **Fig. 3A**, the weight loss of pristine $SiO_2$ NPs, $SiO_2$-PDA, $SiO_2$-PDA-Br and $SiO_2$-PDA-poly(NIPAM) before 100 °C was about 1.72%, 2.05%, 3.12%, and 3.05%, respectively. This should be attributed to the weight loss of water in $SiO_2$ samples. The gradual weight loss of $SiO_2$ NPs was decreased by 3.98% in the range of 100 to 600 °C, which can be considered as the dissociation of tetraethoxysilane on $SiO_2$ NPs. After coated with PDA, the weight loss of $SiO_2$-PDA from the temperature 100 to 600 °C was increased to 9.08%, proving that PDA was successfully coated on the $SiO_2$ NPs via self polymerization of dopamine. Therefore, the weight percentage of PDA coated on the surface of $SiO_2$ NPs could calculate about 5.1% based on the TGA results. Then, for the curve of $SiO_2$-PDA-Br, the weight loss increased to 14.7%, comparing to weight loss of $SiO_2$-PDA (10.8%), the increased percentage of weight loss provided direct evidence of covalent conjugation of initiator to the $SiO_2$-PDA. Later hydrophilic polymers were linked to the surface of $SiO_2$-PDA by the SET-LRP method, the weight loss of functional $SiO_2$ NPs with hydrophilic polymers was increased to 33.4%. Through analyzing of TGA data, the grafted hydrophilic polymers on $SiO_2$ surface was estimated to be 18.7%. These results further demonstrated that $SiO_2$ NPs can be simply modified with hydrophilic polymers

successfully by the combination of mussel inspired chemistry and SET-LRP. The DTA curves of $SiO_2$, $SiO_2$-PDA and $SiO_2$-PDA-Br were shown in **Fig. 3B-E**, they were indicated that an obvious peak was observed between 200 to 300 °C, but the location of the endothermic peak and temperature difference was appeared a slightly different. As shown in **Fig. 3E**, a new endothermic peak is appeared, due to the NIPAM grafting onto $SiO_2$ NPs. The TGA and DTA results powerfully demonstrated that PDA and NIPAM were successfully coated on the $SiO_2$ NPs through combination of mussel inspired chemistry and SET-LRP.

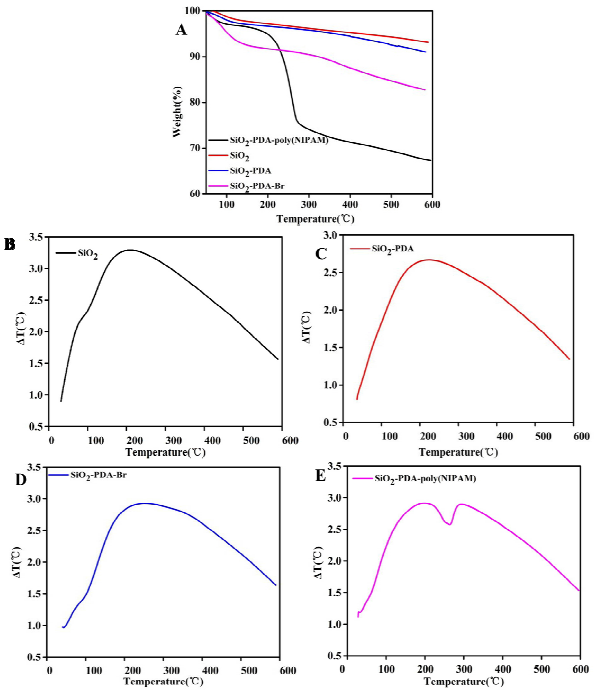


**Fig. 3** TGA curves of $SiO_2$, $SiO_2$–PDA, $SiO_2$–PDA-Br and $SiO_2$–PDA-poly(NIPAM). Significant mass decrease was observed in samples of $SiO_2$-PDA-poly(NIPAM) when the temperature is located at 180-290 °C, indicating the NIPAM was successfully attached on $SiO_2$ NPs via SET-LRP.

The chemical feature of $SiO_2$ NPs, $SiO_2$-PDA, $SiO_2$-PDA-Br, $SiO_2$ -PDA-poly(NIPAM) was confirmed to characterize by XPS spectroscopy. The elements embracing silicon (Si), carbon (C), nitrogen (N), bromine (Br) and oxygen (O) were discovered from XPS spectra (**Fig. 4**). In **Fig. 4A**, we found that three elements including C, Si and O were existed in the sample of primordial $SiO_2$ NPs. It is worth to noting that the information of N1s was emerged in the samples of $SiO_2$-PDA and $SiO_2$-PDA-poly(NIPAM), demonstrating that $SiO_2$ NPs were wrapped with PDA and NIPAM. Then, the track of Br3p was found later in $SiO_2$-PDA-Br. The detailed of O1s, N1s, C1s, Br3p and Si2p XPS spectra were displayed in **Fig. 4B-F**. We are discovered that the binding energy peak of Si in the inchoative $SiO_2$ NPs is exist in 103.17eV, which can be distributed to Si on $SiO_2$ NPs (**Fig. 4B**). After their surface was modified with PDA, the shoulder peaks of C1s moved to the high binding energy between 286.65-286.88 eV (**Fig. 4C**), which was constantly increased in the samples of $SiO_2$-PDA, $SiO_2$-PDA-poly(NIPAM). No surprisingly, the forceful peaks can be attributed to the C-O and C=O bands of PDA and poly(NIPAM). There is a focus on that the peak value of $SiO_2$-PDA-poly(NIPAM) of C1s at high binding energy is much stronger than that of $SiO_2$-PDA, revealing that poly(NIPAM) was grafted onto $SiO_2$-PDA through SET-LRP. The signal of Br3p between 66.45-68.75 eV was only existed in $SiO_2$-PDA-Br (**Fig. 4D**), suggesting that the initiator was successfully immobilized on $SiO_2$-PDA. **Fig. 4E** showed the N1s spectra were detailed in $SiO_2$ samples. The clear N1s peak at 396.2-405.2 eV was appeared in the specimen of $SiO_2$-PDA, proving that PDA was coated on $SiO_2$ NPs. After further modified $SiO_2$-PDA with poly(NIPAM), the tracks of N1s increased appropriately in the samples of $SiO_2$-PDA-poly(NIPAM). From detail information of O1s (**Fig. 4F**), we can see that peak value of O1s exist in 528.10-537.60 eV in the samples of $SiO_2$-PDA and poly(NIPAM) functionalized $SiO_2$ NPs, which are much less than that of pristine $SiO_2$ NPs. And the results are well consistent with the information of C1s and N1s.

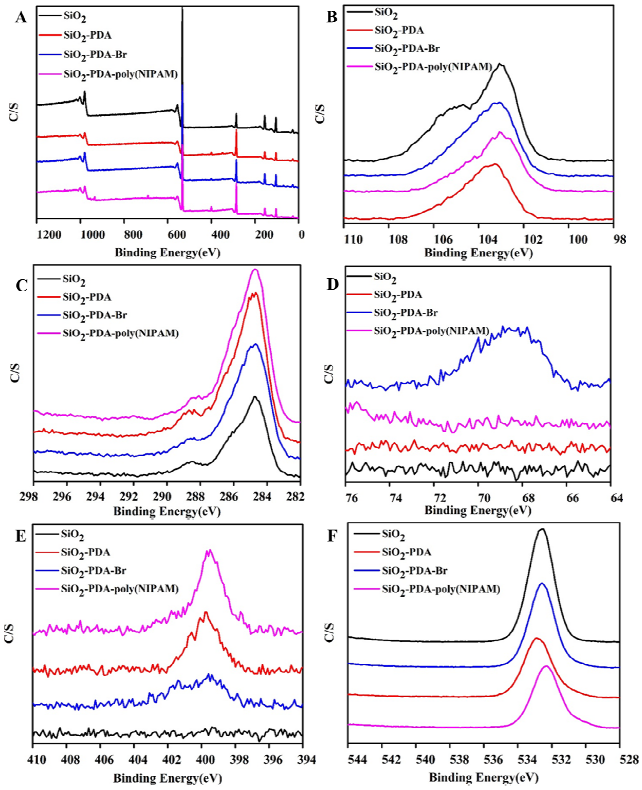


**Fig. 4** (A)The XPS spectra of $SiO_2$, $SiO_2$-PDA , $SiO_2$-PDA-Br and $SiO_2$-PDA-poly(NIPAM).(B) Si2p,(C) C1s, (D) Br3p, (E) N1s and (F) O1s.

In addition, with regard to XPS spectra, the weight percentages of C, N, O, Si were also calculated **(Table 1)**. Three elements Si (17.03%), C (18%) and O (64.97%) were existed in pristine $SiO_2$ NPs. After modifying with PDA, the weight percentages of Si, C and O were changed to 12.54%, 41.43% and 42.68%, respectively. It is worth to mentioning that a new element N (3.35%) was detected in $SiO_2$-PDA. It given strong evidence that $SiO_2$ NPs were successfully modified with PDA through mussel inspired chemistry. However, further modification of $SiO_2$-PDA with poly(NIPAM), the oxygen percentage was decreased to 40.7%. Meanwhile, the most critical point is that the content of N was increased from 3.35% for $SiO_2$-PDA to 4.15% for $SiO_2$-PDA-poly(NIPAM), implying that poly(NIPAM) was grafted

onto $SiO_2$-PDA-Br through SET-LRP.

**Table 1** Element contents (%) of SiO2 NPs based on XPS analysis

| Sample | Si | C | N | O | Br |
|---|---|---|---|---|---|
| SiO2 | 17.03 | 18 | 0 | 64.97 | 0 |
| SiO2-PDA | 12.54 | 41.43 | 3.35 | 42.68 | 0 |
| SiO2-PDA-Br | 15.06 | 28.81 | 1.37 | 53.3 | 1.46 |
| SiO2-PDA-poly(NIPAM) | 12.18 | 41.18 | 4.15 | 42.35 | 0.14 |

The dispersibility is a crucial characteristic in water, which could affect the biomedical applications of nanomaterials, so it was primarily evaluated in detail. As shown in **Fig. S1**, the ungroomed $SiO_2$ NPs were rapidly come down on the bottom of the bottle under 10 min in deionized water. Under the comparison of original $SiO_2$ NPs, the dispersibility of $SiO_2$-PDA in water was improved by coating with PDA, which would subsided within 2 h (**Fig. S1C**), demonstrated the dispersibility was enhanced with PDA. Similarly, when the $SiO_2$-PDA was further modified with poly(NIPAM), the dispersibility of $SiO_2$-PDA-poly(NIPAM) is significantly improved, also explained the $SiO_2$-PDA were modified with poly(NIPAM), No clear solid samples was appeared in the sample of $SiO_2$-PDA-poly(NIPAM) even they were placed for 24 h. It is generally known that poly(NIPAM) is a kind of temperature responsive polymer. The poly(NIPAM) polymer tend to form intramolecular or intermolecular hydrogen bond, which lead to the contraction of molecular chain at higher temperature. So the solubility is reduced in water. On the other hand, the hydrogen bonds can be formed between the poly(NIPAM) polymer and water, which promote molecular chain relaxation at a low temperature, so the solubility is increased in water. The **Fig. 5** showed the solubility of $SiO_2$-PDA-PNIAPAM at different time points at 42 °C. It was found that $SiO_2$-PDA-PNIAPAM was gradually sunk at 42 °C, which was produced a little amount of precipitation at the time point 15 min. And distinct precipitate was observed at 25 min and a vast amounts of sediment was sunk on the bottom of the bottle at 30 min. As compared with previous methods for surface modification of $SiO_2$ NPs, the mussel inspired chemistry described in this work is rather simple and effective. More importantly, due to the photothermal conversion effects, the PDA based nanocomposites may also potentially utilized for laser controlled drug delivery and cancer photothermal treatment.[62]

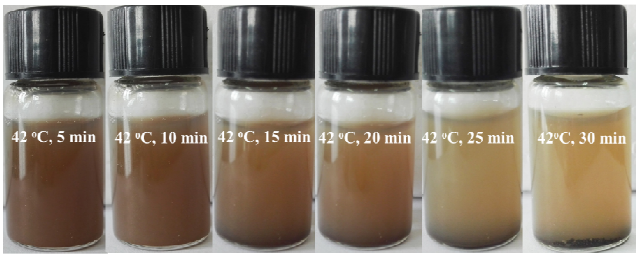


**Fig. 5** The solubility of $SiO_2$-PDA-poly(NIPAM) was assessed in different time points at 42 °C.

## Conclusion

In conclusion, we have developed a novel strategy for surface modification of $SiO_2$ NPs with PDA and poly(NIPAM) by combination of mussel-inspired chemistry and SET-LRP. The successful conjugation of $SiO_2$ NPs with PDA and poly(NIPAM) was demonstrated by a series of characterization techniques including FT-IR spectroscopy, TGA and XPS spectroscopy. Compared with traditional methods for surface functionalization of $SiO_2$ NPs, the method described in this work is rather simple, effective and environmental friendly. Then, the modification method may also be applied for surface modification of many other nanomaterials wih different size, shape and composition. So this method should be a novel and universal strategy for surface modification of nanomaterials and will find potential applications in various fields.

## Acknowledgements

This research was supported by the National Science Foundation of China (Nos. 21134004, 21201108, 51363016, 21474057, 21564006, 21561022), and the National 973 Project (Nos. 2011CB935700).

## Notes

a Department of Chemistry, Nanchang University, 999 Xuefu Avenue, Nanchang 330031, China. b Shaanxi Key Laboratory of Degradable Biomedical Materials, Shaanxi R&D Center of Biomaterials and Fermentation Engineering, School of Chemical and Engineering, Northwest University, Xi'an, 710069, P. R. China; c Department of Chemistry and the Tsinghua Center for Frontier Polymer Research, Tsinghua University, Beijing, 100084, P. R. China.
xiaoyongzhang1980@gmail.com; weiyen@tsinghua.edu.cn; huijunfeng@126.com

† Electronic Supplementary Information (ESI) available: [Dispersibility of silica nanoparticles in water for different time points]. See DOI: 10.1039/b000000x/

## References

1. E. Boisselier and D. Astruc, *Chem. Soc. Rev.*, 2009, **38**, 1759-1782.
2. A. K. Gupta and M. Gupta, *Biomaterials*, 2005, **26**, 3995-4021.
3. N. Ž. Kneževiić, E. Ruiz-Hernández, W. E. Hennink and M. Vallet-Regí, *RSC Adv.*, 2013, **3**, 9584-9593.
4. X. Zhang, K. Wang, M. Liu, X. Zhang, L. Tao, Y. Chen and Y. Wei, *Nanoscale*, 2015, **7**, 11486-11508.
5. X. Zhang, S. Wang, L. Xu, Y. Ji, L. Feng, L. Tao, S. Li and Y. Wei, *Nanoscale*, 2012, **4**, 5581-5584.
6. J. Hui, X. Zhang, Z. Zhang, S. Wang, L. Tao, Y. Wei and X. Wang, *Nanoscale*, 2012, **4**, 6967-6970.
7. X. Zhang, S. Wang, C. Zhu, M. Liu, Y. Ji, L. Feng, L. Tao and Y. Wei, *J. Colloid Interf. Sci.*, 2013, **397**, 39-44.
8. X. Chi, D. Huang, Z. Zhao, Z. Zhou, Z. Yin and J. Gao, *Biomaterials*, 2012, **33**, 189-206.
9. J. Yao, M. Yang and Y. Duan, *Chem. Rev.*, 2014, **114**, 6130-6178.
10. J. Du, M. Liu, X. Lou, T. Zhao, Z. Wang, Y. Xue, J. Zhao and Y. Xu, *Anal. Chem.*, 2012, **84**, 8060-8066.
11. Y.-P. Chen, H.-A. Chen, Y. Hung, F.-C. Chien, P. Chen and C.-Y. Mou, *RSC Adv.*, 2012, **2**, 968-973.
12. S. Jambhrunkar, S. Karmakar, A. Popat, M. Yu and C. Yu, *RSC Adv.*, 2014, **4**, 709-712.
13. X. Zhang, J. Hui, B. Yang, Y. Yang, D. Fan, M. Liu, L. Tao and Y. Wei, *Polym. Chem.*, 2013, **4**, 4120-4125.
14. X. Zhang, S. Wang, C. Fu, L. Feng, Y. Ji, L. Tao, S. Li and Y. Wei, *Polym. Chem.*, 2012, **3**, 2716-2719.
15. X. Zhang, S. Wang, M. Liu, B. Yang, L. Feng, Y. Ji, L. Tao and Y. Wei, *Phys. Chem. Chem. Phys.*, 2013, **15**, 19013-19018.
16. D. Habibi, M. Nasrollahzadeh, L. Mehrabi and S. Mostafaee, *Monatsh. Chem*, 2013, **144**, 725-728.
17. X. Zhang, X. Zhang, B. Yang, L. Liu, J. Hui, M. Liu, Y. Chen and Y. Wei, *RSC Adv.*, 2014, **4**, 10060-10066.
18. X. Zhang, X. Zhang, S. Wang, M. Liu, Y. Zhang, L. Tao and Y. Wei, *ACS Appl. Mater. Interf.*, 2013, **5**, 1943-1947.

19. C. Heng, M. Liu, K. Wang, F. Deng, H. Huang, Q. Wan, J. Hui, X. Zhang and Y. Wei, *Ceram. Int.*, 2015, **41**, 15075-15082.
20. C. Zhu, L. Liu, Q. Yang, F. Lv and S. Wang, *Chem. Rev.*, 2012, **112**, 4687-4735.
21. S. K. Natarajan and S. Selvaraj, *RSC Adv.*, 2014, **4**, 14328-14334.
22. X. Huang, T. Zhang, A. Goswami, F. Luo and T. Asefa, *RSC Adv.*, 2015, **5**, 28836-28839.
23. G. Shi, Y. Mao, G. Ren, L. Gong and Z. Zhi, *Opt. Commun*, 2014, **332**, 219-222.
24. J. Wang, C. Xu, B. Shen and J. Zhai, *J. Mater. SCI. Mater. El*, 2013, **24**, 3309-3314.
25. F. Wang, G. M. Pauletti, J. Wang, J. Zhang, R. C. Ewing, Y. Wang and D. Shi, *Adv. Mater*, 2013, **25**, 3485-3489.
26. Z. Han, L. Wang, J. Zhu, S. Zhang and W. Zhou, *J. Appl. Polym. Sci*, 2011, **122**, 43-49.
27. N. Zhang, S. R. Samanta, B. M. Rosen and V. Percec, *Chem. Rev.*, 2014, **114**, 5848-5958.
28. L. Bai, L. Zhang, Z. Cheng and X. Zhu, *Polym. Chem.*, 2012, **3**, 2685-2697.
29. A. H. Soeriyadi, C. Boyer, F. Nystro?m, P. B. Zetterlund and M. R. Whittaker, *J. Am. Chem. Soc.*, 2011, **133**, 11128-11131.
30. X. Hu, J. Li, H. Li and Z. Zhang, *J. Polym. Sci. Pol. Chem*, 2012, **50**, 3126-3134.
31. V. Percec, T. Guliashvili, J. S. Ladislaw, A. Wistrand, A. Stjerndahl, M. J. Sienkowska, M. J. Monteiro and S. Sahoo, *J. Am. Chem. Soc.*, 2006, **128**, 14156-14165.
32. Y. Deng, Y. Li, J. Dai, M. Lang and X. Huang, *J. Polym. Sci. Polym. Chem.*, 2011, **49**, 4747-4755.
33. Y. Deng, J. Z. Zhang, Y. Li, J. Hu, D. Yang and X. Huang, *J. Polym. Sci. Polym. Chem.*, 2012, **50**, 4451-4458.
34. A. Ding, G. Lu, H. Guo, X. Zheng and X. Huang, *J. Polym. Sci. Polym. Chem.*, 2013, **51**, 1091-1098.
35. S. Zhai, J. Shang, D. Yang, S. Wang, J. Hu, G. Lu and X. Huang, *J. Polym. Sci. Polym. Chem.*, 2012, **50**, 811-820.
36. Q. Wan, M. Liu, J. Tian, F. Deng, Y. Dai, K. Wang, Z. Li, Q. Zhang, X. Zhang and Y. Wei, *RSC Adv.*, 2015, **5**, 38316-38323.
37. L. Bai, L. Zhang, J. Pan, J. Zhu, Z. Cheng and X. Zhu, *Macromolecules*, 2013, **46**, 2060-2066.
38. J. Xu, K. Jung and C. Boyer, *Macromolecules*, 2014, **47**, 4217-4229.
39. C. A. Bell, Z. Jia, J. Kulis and M. J. Monteiro, *Macromolecules*, 2011, **44**, 4814-4827.
40. Y. Xie, C. He, L. Liu, L. Mao, K. Wang, Q. Huang, M. Liu, Q. Wan, F. Deng and H. Huang, *RSC Adv.*, 2015, **5**, 82503-82512.
41. J. Tian, D. Xu, M. Liu, F. Deng, Q. Wan, Z. Li, K. Wang, X. He, X. Zhang and Y. Wei, *J. Polym. Sci. Polym. Chem*, 2015.
42. X. Zhang, Q. Huang, M. Liu, J. Tian, G. Zeng, Z. Li, K. Wang, Q. Zhang, Q. Wan and F. Deng, *Appl. Surf. Sci*, 2015, **343**, 19-27.
43. Q. Wan, M. Liu, J. Tian, F. Deng, G. Zeng, Z. Li, K. Wang, Q. Zhang, X. Zhang and Y. Wei, *Polym. Chem.*, 2015, **6**, 1786-1792.
44. L. Li, W. Smitthipong and H. Zeng, *Polym. Chem.*, 2015, **6**, 353-358.
45. M. A. Matin, R. K. Chitumalla, M. Lim, X. Gao and J. Jang, *J Phys. Chem. B*, 2015, **119**, 5496-5504.
46. N. Bandara, H. Zeng and J. Wu, *J Adhes. Sci.Technol*, 2013, **27**, 2139-2162.
47. C. E. Brubaker and P. B. Messersmith, *Langmuir*, 2012, **28**, 2200-2205.
48. Y. Cao, X. Zhang, L. Tao, K. Li, Z. Xue, L. Feng and Y. Wei, *ACS Appl. Mater. Interf.*, 2013, **5**, 4438–4442.
49. L. Xu, N. Liu, Y. Cao, F. Lu, Y. Chen, X. Zhang, L. Feng and Y. Wei, *ACS Appl. Mater. Interf.*, 2014, **6**, 13324-13329.
50. H. Lee, S. M. Dellatore, W. M. Miller and P. B. Messersmith, *science*, 2007, **318**, 426-430.
51. L. Q. Xu, W. J. Yang, K.-G. Neoh, E.-T. Kang and G. D. Fu, *Macromolecules*, 2010, **43**, 8336-8339.
52. F. Meng, W. E. Hennink and Z. Zhong, *Biomaterials*, 2009, **30**, 2180-2198.
53. L. Wong, S. Sevimli, H. M. Zareie, T. P. Davis and V. Bulmus, *Macromolecules*, 2010, **43**, 5365-5375.
54. X. Zhang, J. Ji, X. Zhang, B. Yang, M. Liu, W. Liu, L. Tao, Y. Chen and Y. Wei, *RSC Adv.*, 2013, **3**, 21817-21823.
55. X. Zhang, M. Liu, Y. Zhang, B. Yang, Y. Ji, L. Feng, L. Tao, S. Li and Y. Wei, *RSC Adv.*, 2012, **2**, 12153-12155.
56. Q. Wan, J. Tian, M. Liu, G. Zeng, Z. Li, K. Wang, Q. Zhang, F. Deng, X. Zhang and Y. Wei, *RSC Adv.*, 2015, **5**, 25329-25336.
57. X. Zhang, Q. Huang, M. Liu, J. Tian, G. Zeng, Z. Li, K. Wang, Q. Zhang, Q. Wan and F. Deng, *Appl. Surf. Sci.*, 2015, **343**, 19-27.
58. Y. Xie, Q. Huang, M. Liu, K. Wang, Q. Wan, F. Deng, L. Lu, X. Zhang and Y. Wei, *RSC Adv.*, 2015, **5**, 68430-68438.
59. Q. Wan, L. Mao, M. Liu, K. Wang, G. Zeng, D. Xu, H. Huang, X. Zhang and Y. Wei, *Polym. Chem.*, 2015, **6**, 7211-7218.
60. L. Fu, Y. Shi, K. Wang, P. Zhou, M. Liu, Q. Wan, L. Tao, X. Zhang and Y. Wei, *New J. Chem.*, 2015, DOI: 10.1039/C1035NJ02055G
61. M. Liu, J. Ji, X. Zhang, X. Zhang, B. Yang, F. Deng, Z. Li, K. Wang, Y. Yang and Y. Wei, *J. Mater. Chem. B*, 2015, **3**, 3476-3482.
62. Y. Liu, K. Ai, J. Liu, M. Deng, Y. He and L. Lu, *Adv. Mater.*, 2013, **25**, 1353-1359.